2010

Geobacter uraniireducens NikR Displays a DNA binding mode distinct from other members of the NikR family

Erin L. Benanti
Washington University School of Medicine in St. Louis
Peter T. Chivers
Washington University School of Medicine in St. Louis

JOURNAL OF BACTERIOLOGY, Sept. 2010, p. 4327–4336 Vol. 192, No. 17
0021-9193/10/$12.00 doi:10.1128/JB.00152-10

Geobacter uraniireducens NikR Displays a DNA Binding Mode Distinct from Other Members of the NikR Family▽†

Erin L. Benanti and Peter T. Chivers*

Department of Biochemistry and Molecular Biophysics, Washington University School of Medicine, St. Louis, Missouri 63110

Received 12 February 2010/Accepted 12 June 2010

NikR is a nickel-responsive ribbon-helix-helix transcription factor present in many bacteria and archaea. The DNA binding properties of *Escherichia coli* and *Helicobacter pylori* NikR (factors EcNikR and HpNikR, respectively) have revealed variable features of DNA recognition. EcNikR represses a single operon by binding to a perfect inverted repeat sequence, whereas HpNikR binds to promoters from multiple genes that contain poorly conserved inverted repeats. These differences are due in large part to variations in the amino acid sequences of the DNA-contacting β-sheets, as well as residues preceding the β-sheets of these two proteins. We present here evidence of another variation in DNA recognition by the NikR protein from *Geobacter uraniireducens* (GuNikR). GuNikR has an Arg-Gly-Ser β-sheet that binds specifically to an inverted repeat sequence distinct from those recognized by Ec- or HpNikR. The N-terminal residues that precede the GuNikR β-sheet residues are required for high-affinity DNA binding. Mutation of individual arm residues dramatically reduced the affinity of GuNikR for specific DNA. Interestingly, GuNikR tetramers are capable of binding cooperatively to the promoter regions of two different genes, *nik(MN)1* and *nik(MN)2*. Cooperativity was not observed for the closely related *G. bemidjiensis* NikR, which recognizes the same operator sequence. The cooperative mode of DNA binding displayed by GuNikR could affect the sensitivity of transporter gene expression to changes in intracellular nickel levels.

Approximately 60% of the bacterial and 85% of the archaeal sequenced genomes encode nickel-dependent enzymes (49). Across these microbes, there are at least nine nickel-dependent enzymes that are integral to energy generation, nitrogen assimilation and detoxification, including [Ni-Fe] hydrogenase, methyl CoM-reductase, carbon monoxide dehydrogenase (CODH), urease, and Ni-superoxide dismutase (31). Notably, the numbers and combinations of nickel-dependent enzymes in each species vary significantly, which likely reflects the disparate growth environments and lifestyles of microorganisms.

A previous survey of the prevalence of nickel transporters (35) indicated that most nickel-utilizing organisms also encode identifiable nickel transporters. This analysis used the presence of the Ni^{2+}-dependent transcription factor NikR (11, 15, 18, 46, 49) in sequenced genomes and predicted NikR operators to identify candidate nickel transporter genes. Based on the present study, NikR likely regulates a variety of nickel transporters in many different organisms, including the NikMNQO (10, 35) and NikABCDE (32) ABC-type transporters, as well as the HupE/UreJ and nickel-cobalt permeases (35). Together with the mosaic distribution of nickel-dependent enzymes, these observations raise the question of whether the regulatory properties of different NikR orthologs are modulated in response to different microbial nickel physiologies.

NikR is a tetramer that consists of an N-terminal ribbon-helix-helix (RHH; or β-α-α) DNA binding domain (11) and a C-terminal metal-binding domain (MBD) that binds Ni^{2+} with high affinity (11–13, 39, 40). Nickel binding to the MBD activates NikR to bind to specific DNA sequences and regulate gene expression (1, 6, 8, 13, 23, 27). *Escherichia coli* NikR (EcNikR) was the first member of this large family of transcription factors to be studied (11, 18), and its function is relatively well understood (11, 13, 18, 27, 36, 46). Subsequent studies have examined the biology and biochemical properties of *Helicobacter pylori* NikR (HpNikR). Although the primary nickel binding properties are conserved, HpNikR DNA recognition is distinct from EcNikR (1, 5, 6, 15–17, 19–20, 22, 23).

NikR, as for all RHH family members, makes base-specific DNA contacts via antiparallel β-sheets at its N terminus (34, 40). Residues N terminal to the β-sheet ("N-terminal arms") of RHH proteins make nonspecific DNA phosphate contacts (7, 34, 42). EcNikR binds to a perfect inverted repeat in the promoter of the *nikABCDE* operon (13), whereas HpNikR recognizes poorly conserved imperfect inverted repeats in the promoters of multiple repressed and activated genes (1, 6, 17, 20, 22). The nine residue N-terminal arm of HpNikR, which is absent in EcNikR, is required to maintain the hierarchy of affinities this ortholog displays for different promoters (6) and to inhibit nonspecific DNA binding (6, 28). It remains to be determined whether the differences in DNA binding activity of EcNikR and HpNikR are further indicative of a spectrum of DNA binding affinities and specificities throughout the NikR family. Significant variation in β-sheet residues and N-terminal arm lengths and sequences exist within the NikR family (6), suggesting that differences in N-terminal amino acid sequence allow variation in the protein-DNA interface that influence the regulatory properties of NikR.

We have initiated studies of a third NikR protein (GuNikR) from the Gram-negative deltaproteobacteria *Geobacter urani-*

* Corresponding author. Mailing address: Department of Biochemistry and Molecular Biophysics, Box 8231, Washington University School of Medicine, 660 S. Euclid Ave., St. Louis, MO 63110. Phone: (314) 362-1496. Fax: (314) 362-7183. E-mail: chivers@wustl.edu.

† Supplemental material for this article may be found at http://jb.asm.org/.

▽ Published ahead of print on 25 June 2010.

ireducens strain Rf4 (41) to better understand how protein-DNA interactions vary across the NikR family. GuNikR was chosen in part because it contains distinct N-terminal arm and β-sheet sequences relative to EcNikR and HpNikR. *Geobacter* species carry out dissimilatory metal reduction and can use molecular hydrogen as a source of electrons for this process (29). *G. uraniireducens* Rf4 was initially isolated from a uranium bioremediation field site, where its presence was associated with an increase in Fe(III) reduction and a decrease in U(VI) concentrations (3). The combination of nickel-dependent enzymes encoded in the *G. uraniireducens* Rf4 genome (six [Ni-Fe] hydrogenase enzymes and one CODH [http://www.ncbi.nlm.nih.gov/nuccore/CP000698]) is unique from those of *Escherichia coli* (four hydrogenases) (4, 37, 45) and *H. pylori* (hydrogenase, urease) (44). There is one predicted *nik(MN)QO* operon in *G. uraniireducens*, as well as a second *nik(MN)* gene located near the *nikR* gene. [*nik(MN)* refers to a fusion of the *nikMN* genes that was described previously (35)].

Our results reveal several new aspects of NikR-DNA interactions, including the experimental verification of a previously predicted NikR DNA recognition motif (35) that is present in two *G. uraniireducens nik(MN)* promoter regions and conserved across *Geobacter* species. GuNikR showed nickel-responsive repression of $P_{nik(MN)}$-*lacZ* fusion reporters in *E. coli*. Interestingly, GuNikR tetramers bind with strong positive cooperativity to one *nik(MN)* promoter candidate. Deletion and site-directed mutagenesis demonstrated that the GuNikR N-terminal arm is absolutely required for DNA binding and individual arm residues contribute to high-affinity DNA binding, as well as cooperativity in some cases.

MATERIALS AND METHODS

Bioinformatics. The *H. pylori* 26695 NikR protein sequence (HP1338) was used in a protein BLAST (2) search of the NCBI nonredundant protein sequence database (performed in April 2009). Hits with significant similarity (minimum score of 100) were filtered for redundant sequences and then screened for the presence of the four high-affinity Ni^{2+}-binding site ligands (EcNikR numbering: His76, His87, His89, and Cys95 [39]). β-Sheet sequences plus any amino acids N-terminal to the β-sheet were then filtered to remove redundant sequences (100% identity) and aligned by using CLUSTAL W (43).

Cloning and mutagenesis of *Geobacter nikR* genes. Genomic DNA from *G. uraniireducens* (Evgenya Shelobolina, University of Wisconsin, Madison) and *G. bemidjiensis* (Derek Lovley; University of Massachusetts-Amherst) was used to amplify *nikR* by PCR using the primers listed in Table S1 in the supplemental material (Invitrogen, Carlsbad, CA). Digested PCR products were cloned into pET22-b by using the NdeI and XhoI restriction sites (Novagen, Madison, WI) to generate pEB270 and pEB259 (see Table S1 in the supplemental material). Δnt3GuNikR was constructed by using the primers EB499 and EB470 to amplify a 5′ truncated *nikR* gene using pEB270 as a template. The resulting product was cloned as described above to generate pEB296. Site-directed mutagenesis of individual GuNikR residues was carried out by using the QuikChange site-directed mutagenesis protocol (Stratagene, La Jolla, CA) using complementary oligonucleotides with the mutated codon (see Table S1 in the supplemental material) and *Pfu* DNA polymerase. The DNA sequence of each construct was verified by sequencing (SeqWright, Houston, TX).

Protein purification and expression. Wild-type and mutant NikR proteins were expressed and purified as described previously for EcNikR (12, 13) except that sequential steps of Q-Sepharose ion exchange (20 mM Tris-HCl [pH 8.0] 50 mM to 1 M NaCl gradient) and gel filtration (20 mM Tris-HCl [pH 8.0] and 300 mM NaCl) were performed after Ni-NTA chromatography. The protein concentration was determined in 6 M guanidine hydrochloride (GuHCl) using ε_{280} = 8,480 M^{-1} cm^{-1}, as predicted by primary sequence analysis (25). To remove Ni^{2+} from the purified proteins, the Ni-NTA eluate was incubated with 20 mM L-histidine for 24 h at 4°C, followed by ion exchange and gel filtration (the second and third purification steps). The removal of Ni^{2+} was confirmed by the absence of any UV-visible absorbance at 304 nm.

Candidate binding site fragments: cloning and labeling. Candidate NikR binding site fragments were amplified from genomic DNA by PCR using the oligonucleotide pairs listed in Table S1 in the supplemental material. Mutant $P_{nik(MN)1}$ fragments were constructed by two successive rounds of PCR using internal primers containing the scrambled repeats. For the site 1 mutant, PCR products from reactions using the primer pairs EB687-EB690 and EB683-EB682 were mixed and used as the template in a second round of PCR using the external primers EB687/EB682 (see Table S1 in the supplemental material). The site 2 mutant was made using the same strategy, except with the primers EB689 and EB685 in place of EB690 and EB683, respectively. The resulting PCR products were digested with EcoRI and KpnI and ligated into pBluescript II KS (Stratagene) to generate pEB319 and pEB320. Cloned promoter candidates were verified by sequencing (Seqwright).

DNA fragments for binding assays were labeled as previously described by a combination of end labeling one primer and PCR amplification (6) or by end filling an EagI-digested PCR promoter fragment. End-fill reactions used 0.2 μM PCR product, Klenow fragment DNA polymerase (3′-5′ exo^-; NEB, Beverly, MA), and [α-^{32}P]dGTP (GE Biosciences, Piscataway, NJ) in a total volume of 40 μl. Excess [α-^{32}P]dGTP was removed by using a nucleotide exchange kit (Qiagen, Valencia, CA). When necessary, labeled DNA fragments were further purified by acrylamide gel electrophoresis.

DNA binding assays. DNase I footprinting was performed as described previously (6) in a binding buffer containing 10 mM Tris-HCl (pH 8.0), 100 mM KCl, 3 mM $MgCl_2$, 10 mg of *E. coli* thioredoxin/liter, and 4 mg of salmon sperm DNA (Fisher)/liter. $NiCl_2$ was added as described in the text and figure legends. Labeled DNA fragments were incubated with protein (22°C for 30 min) prior to DNase I addition (final concentration, 300 ng/ml; Sigma). Formic acid cleavage of labeled DNA was performed by using the standard protocol for Maxam-Gilbert sequencing (21).

Electrophoretic mobility shift assays (EMSAs; 7% polyacrylamide gel) were performed as previously described (6) using a dilution series of at least 15 protein concentrations. The binding buffer was identical to that used for DNase I footprinting except with 50 μM $NiCl_2$.

Apparent affinities from DNase I footprinting and mobility shift assays were calculated by using the Hill equation as previously described (6). The reported values and calculated standard deviations are the average of two or more independent experiments.

Promoter-*lacZ* reporter assays. $P_{nik(MN)1}$ and $P_{nik(MN)2}$ promoter fragments were amplified from genomic DNA by PCR using the oligonucleotide pairs listed in Table S1 in the supplemental material. The purified PCR fragments were digested with EagI and SalI and cloned into pPC163 (13) digested with the same enzymes. pPC163 contains the *E. coli* lacZ gene fused to the $P_{nikABCDE}$ promoter and has been used to study EcNikR activity. For LacZ assays, the reporter plasmids were transformed into PC606, a Δ*lacZ* derivative of *E. coli* DL41(DE3)Δ*metA*. The resulting cells were transformed with either pEB270 or pNIK103 (13), which contains a copy of *E. coli nikR*. Cells were grown aerobically in M63 minimal medium containing 20 μg of L-methionine/ml in the absence or presence of $NiCl_2$ (3 μM). IPTG (isopropyl-β-D-thiogalactopyranoside) was not added to the growth medium. LacZ assays were performed as described previously (11, 13, 18, 27, 36, 46).

RESULTS

N-terminal sequence variation in the NikR family. The alignment of 74 NikR orthologs with nonidentical N-terminal amino acid sequences (see Materials and Methods and Fig. S1 in the supplemental material) revealed a high degree of variability in β-sheet and arm sequence, as well as in arm length. The specific variations are described below.

β-Sheet sequences. Nine different combinations of DNA-contacting β-sheet residues were identified (Fig. 1a). Over half of the predicted NikR proteins contained Arg-Gly-Ser and Arg-Ser-Ser sequences (37 and 22 of the 74 sequences, respectively; Fig. 1a and b). Arginine is almost always conserved at the first position (Fig. 1b). The only exception is a Lys substitution in *Staphylothermus marinus* NikR. In contrast, five different amino acids occur at the second and third positions (Fig.

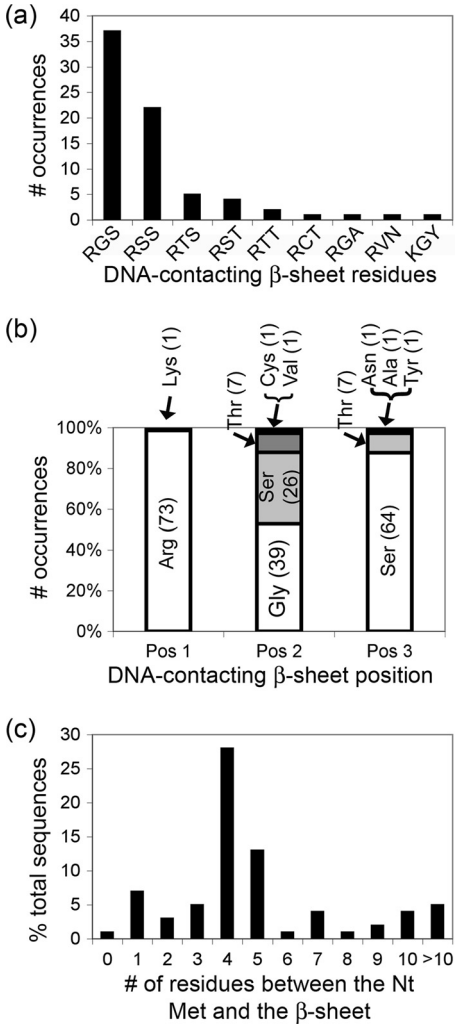

FIG. 1. Frequency of DNA-contacting β-sheet sequences and N-terminal arm lengths among nonidentical NikR homologs. (a) The number of NikR proteins containing one of nine combinations of DNA-contacting β-sheet residues. (b) The relative percentage of each residue occurring at each β-sheet position. The total number of sequences with each residue is noted in parentheses. (c) The number of NikR proteins containing increasing numbers of residues between the N-terminal (Nt) Met and the first DNA-contacting β-sheet residue.

1b). These residues are generally small and not always capable of direct interactions with DNA bases. Glycine is present at the second position in roughly half of the sequences, but is never found in the third position. Serine is the next most common at the second position and most common at the third position.

The high degree of conservation of Arg at the first position is not surprising. In EcNikR, this residue makes four of the five specific base interactions observed in the DNA cocrystal structure (40). The other base-specific contact observed in the EcNikR cocrystal structure occurs via Thr5, the second DNA-contacting sheet position (40). This suggests that different specific DNA contacts may occur in Arg-Gly-Ser NikR proteins to compensate for the likely absence of a DNA interaction at this position or that additional nonspecific contacts may be present. In either case, the sequence composition of the inverted repeats of the DNA binding site is expected to change.

N-terminal arm length variation. Comparison of the number of residues occurring between the N-terminal Met and the first position of the β-sheet of each NikR protein indicated that N-terminal arm lengths range from 0 to 32 amino acids, with the largest number of homologs containing four or five amino acids between Met1 and the β-sheet Arg (43 of 79 sequences; Fig. 1c). There was no obvious correlation between N-terminal arm length and β-sheet sequence, except that the arms of the RTT β-sheet sequences were generally shorter. An important qualification is that the NikR sequences analyzed here are based on genome annotations, so some particularly long NikR arms may result from an incorrect annotation of the *nikR* start codon or a sequencing error (see Fig. S1 in the supplemental material).

The lack of experimental information on the largest NikR subgroup (Arg-Gly-Ser β-sheet) that exhibits wide variation in arm length led us to investigate the DNA binding properties of members of this subgroup. To this end, several NikR proteins with Arg-Gly-Ser β-sheets and different arm sequences were cloned, overexpressed in *E. coli*, purified, and screened for DNA binding activity (E. L. Benanti and P. T. Chivers, unpublished data). We focused on GuNikR based on the ease of obtaining sufficient quantities of protein for these studies and the identification of potential DNA binding sites (Fig. 2a).

GuNikR purification and nickel binding. GuNikR was purified by using a protocol similar to that used for EcNikR (11) and HpNikR (1, 6). GuNikR eluted from a size exclusion column at a volume consistent with an ~60-kDa tetramer (data not shown), the same oligomeric state as EcNikR (12) and HpNikR (1, 28). The UV-visible difference spectrum of the protein with or without stoichiometric Ni(II) showed the characteristic features seen for EcNikR (13) and HpNikR (1, 6). The far UV circular dichroism (CD) spectrum of GuNikR was consistent with that observed for EcNikR (13). The CD spectrum did not change significantly with the addition of stoichiometric $NiCl_2$ (see Fig. S2 in the supplemental material). Chemical denaturation of the apo- and holoproteins revealed an increase in stability in the presence of nickel (see Fig. S2 in the supplemental material), demonstrating that GuNikR directly binds nickel, consistent with the UV-visible spectrum. These properties of GuNikR were expected based on the shared characteristics previously observed for Ec- and HpNikR.

DNA binding site prediction. Nickel- or NikR-dependent gene regulation has not been studied in *G. uraniireducens*. However, GuNikR likely represses genes encoding putative nickel transporters, as observed for EcNikR and HpNikR (11, 16, 18, 22, 23). This expectation was used previously to predict different NikR binding site motifs (35). We used the results of that study to scan the *G. uraniireducens* genome for potential NikR-regulated nickel transporter genes. BLASTP searches (2) of the *G. uraniireducens* genome with the *Rhodococcus capsulatus* Nik(MN) protein sequence identified two genes, Gura0780 and Gura2762 (27 and 24% identical to *R. capsulatus* NikMN, respectively, and 84% identity with each other). Homology searches with other types of nickel transporters did not return any meaningful candidate genes.

Gura0780 and Gura2762 are both annotated as CbiM-encoding genes, which are cobalt-specific ABC-type transporter proteins analogous to Nik(MN) (35). We refer to Gura0780 as

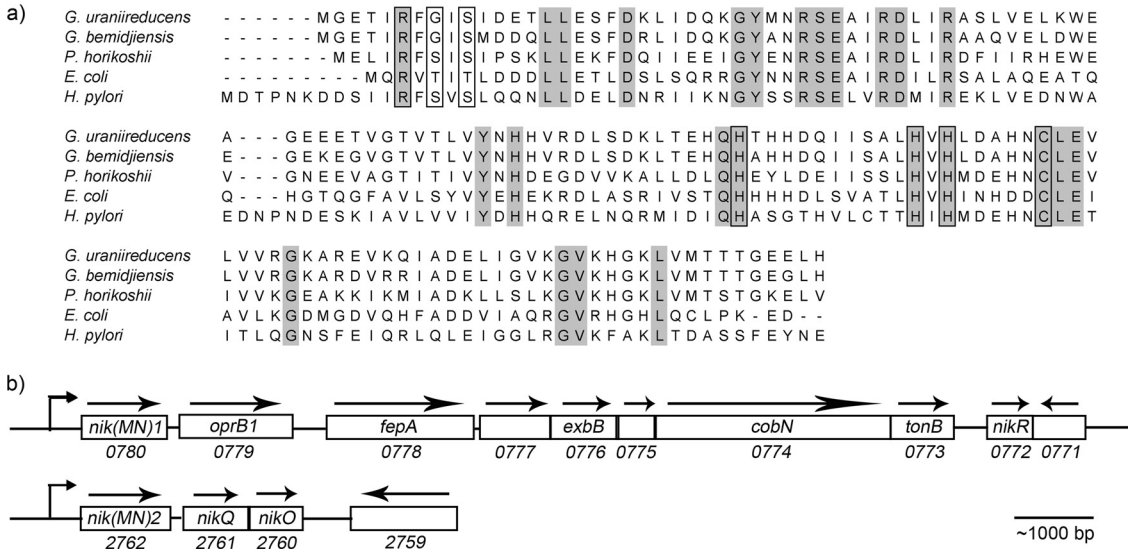

FIG. 2. Distinct N terminus of GuNikR and its predicted target genes. (a) CLUSTAL W multiple sequence alignment of NikR proteins from *G. uraniireducens*, *G. bemidjiensis*, *Pyrococcus horikoshii*, *E. coli*, and *H. pylori*. Residues conserved in all four proteins are shaded gray, and DNA-contacting β-sheet residues and high-affinity Ni^{2+} binding site ligands are boxed. (b) Schematic of the *G. uraniireducens nik(MN)1* and *nik(MN)2* chromosomal loci. The candidate promoters of each *nik(MN)* gene are indicated. Genes are indicated by their gene number and the name of their best BLAST hit, if a putative homolog exists. The arrows indicate gene orientation. There are 606 bp between the Gura0779 and Gura0778 genes and 263 bp between Gura0773 and *nikR*. An RNA polymerase sigma subunit consensus recognition sequence (TTGACA) is present in these intergenic regions, suggesting that they can be transcribed independently of *nik(MN)1*.

nik(MN)1 based on the gene regulatory criteria used to identify *R. capsulatus* Nik(MN) (35) and the results described below. *nik(MN)1* is located upstream of eight additional genes that encode TonB (Gura0773), TonB-related membrane proteins, and NikR itself (Gura0772; Fig. 2b). TonB functions to energize the transport of iron complexes across the outer membrane (33) but has recently been linked to nickel transport in *H. pylori* under acidic growth conditions (38). There are two relatively large intergenic distances within this region, and the presence of putative −35 TTCAGA consensus elements in these regions suggests that they may be transcribed independently. Gura2762 [*nik(MN)2*] is the first gene of a *nik(MN)QO* operon located at a site ~2 Mb away from *nik(MN)1* on the chromosome.

GuNikR binds specifically to two *nik(MN)* promoter regions. Candidate fragments upstream of *nik(MN)1* and *nik(MN)2* were tested for DNA binding by GuNikR. GuNikR binding to a DNA fragment spanning the ~260-bp region between nikR and the closest upstream gene (Fig. 2b) was also tested. In addition, versions of the predicted NikR recognition motif (35), which exists in the sequences immediately upstream of both *nik(MN)* genes, occur in the upstream regions of the *G. uraniireducens fur* and *hypE* genes. *fur* encodes an iron-dependent transcription factor, which is regulated by NikR in *H. pylori* (15, 17), and *hypE* encodes a [Ni-Fe] hydrogenase chaperone. GuNikR bound only to the *nik(MN)1* and *nik(MN)2* upstream regions (Fig. 3a), as detected by EMSA. No binding was detected to the *nikR*, *fur*, or *hypE* upstream DNA fragments (data not shown). The mobility shifts required the presence of 50 μM $NiCl_2$ in the gel and running buffer, which has been observed previously for other NikR proteins (1, 6, 13). Binding was not detected with 1 mM $MgCl_2$, which can substitute for $NiCl_2$ in EMSAs with HpNikR (6). The absence of detectable binding to the *nikR*, *fur*, and *hypE* upstream regions indicates that GuNikR binding to the *nik(MN)* upstream regions is sequence specific. Titrations of GuNikR with $P_{nik(MN)1}$ and $P_{nik(MN)2}$ revealed apparent affinities of 8 and 64 nM, with Hill coefficients of 1.6 and 0.6, respectively (Fig. 3a and Table 1).

The *nik(MN)1* and *nik(MN)2* mobility shifts had distinct features. In both cases, the DNA fragments qualitatively showed a larger mobility shift in the presence of GuNikR compared to EMSA studies of other NikR proteins (1, 6, 13). Furthermore, an intermediate shifted species was observed for $P_{nik(MN)2}$ but not $P_{nik(MN)1}$ (Fig. 3a), suggesting that GuNikR may bind to both candidate promoters with more than one tetramer present in the shifted complex.

$P_{nik(MN)1}$ and $P_{nik(MN)2}$ are functional and nickel responsive. The candidate *nik(MN)* promoter fragments were cloned upstream of the *E. coli lacZ* gene to test for nickel-dependent expression. Both constructs were functional in *E. coli* (Fig. 4). Nickel-dependent repression of LacZ expression was observed for both $P_{nik(MN)1}$ and $P_{nik(MN)2}$ reporters when a plasmid constitutively expressing a low level of GuNikR was also present (Fig. 4). No nickel responsive regulation was observed in the presence of a plasmid encoding EcNikR. The difference in expression in the absence of added nickel between GuNikR- and EcNikR-containing cells also distinguishes between functional and nonfunctional NikRs in this assay, as has been demonstrated previously for EcNikR (36). The activity of GuNikR in this case is likely due to trace nickel in the M63 minimal medium.

GuNikR binds cooperatively to the *nik(MN)* promoters. The GuNikR-DNA complexes were further investigated by using DNase I footprinting. In the presence of stoichiometric (1:1) $NiCl_2$, GuNikR protected a 70-bp region of $P_{nik(MN)1}$ (Fig. 5a).

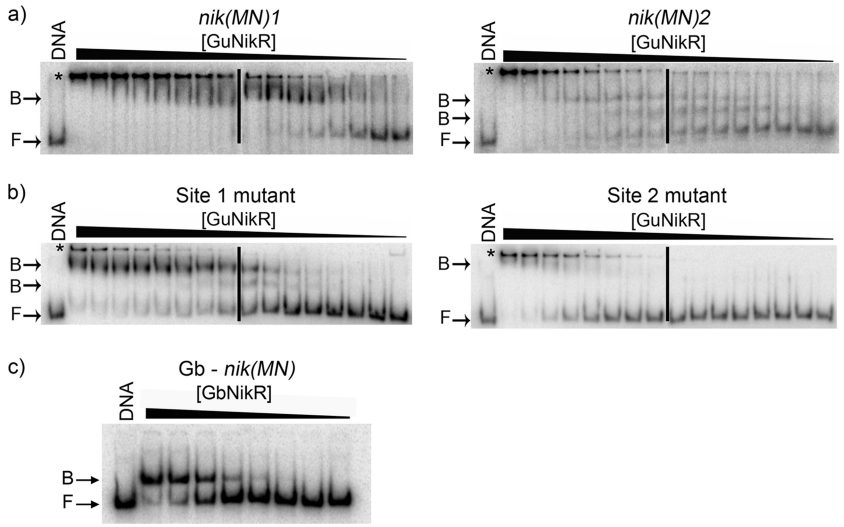

FIG. 3. Two GuNikR tetramers bind to two *nik(MN)* candidate promoters. GuNikR was serially diluted 1.7-fold from 5.0 μM to 17.5 nM with (a) $P_{nik(MN)1}$ (left panels) or $P_{nik(MN)2}$ (right panels) and (b) $P_{nik(MN)1}$ site 1 (left panels) and site 2 (right panels) mutant promoter fragments. (c) GbNikR was serially diluted 3-fold from 5.0 μM to 2.3 nM with *G. bemidjiensis* $P_{nik(MN)}$. Mobility shifts were performed with 50 μM $NiCl_2$ in the gel and running buffer. Each full titration was run on two separate gels in parallel, and a vertical line separates each pair of gel images. F, free DNA. B, protein-bound DNA. The asterisk indicates DNA in wells.

The sequence features of this region are discussed in more detail below. This protection was roughly twice the size of that reported for EcNikR (8, 12) and HpNikR (1, 6, 17, 22) under similar conditions, and fits of DNase I GuNikR titrations indicated a Hill coefficient of 2.03 (Table 1). Together, these results suggest that two GuNikR tetramers bind to $P_{nik(MN)1}$. In contrast, the GuNikR-dependent DNase I footprint of $P_{nik(MN)2}$ was roughly 33 bp in the presence of stoichiometric or 50 μM $NiCl_2$, which is similar to the size of the protection pattern observed for EcNikR and HpNikR. However, the Hill coefficient of 2.56 determined for GuNikR binding to $P_{nik(MN)2}$ in this assay indicates positive cooperativity (Table 1). In the absence of any nickel and in the presence of 50 μM EDTA, the affinity of GuNikR for $P_{nik(MN)1}$ decreased ~5-fold (K_D of 88 nM; data not shown), a finding consistent with nickel-dependent activation of DNA binding.

Based on the appearance of the footprinting and mobility shift data, the GuNikR-$P_{nik(MN)1}$ interaction likely involves two NikR tetramers bound to one DNA fragment. This model is supported by Hill coefficients of >1 required to fit both sets of data (Table 1). The affinities of the two interactions differed by 2-fold (K_D = 7.6 nM versus 16.5 nM for mobility shift and footprint, respectively).

In contrast, the GuNikR-$P_{nik(MN)2}$ mobility shift data could not be fit well using a simple two-site interaction model. This was due both to the persistence of the intermediate shifted species suggestive of negative cooperativity and the presence of multiple additional binding sites with different and weaker affinities. The lack of a defined second binding site for $P_{nik(MN)2}$ is consistent with the absence of an extended DNase I footprint for the GuNikR-$P_{nik(MN)2}$ interaction, which could result from multiple secondary binding sites with reduced affinities (see below) or two tetramers binding on the opposite face of the same stretch of DNA. The Hill coefficient of 2 determined for GuNikR binding to $P_{nik(MN)2}$ suggests a positively cooperative interaction. The affinity of GuNikR for $P_{nik(MN)2}$ measured by DNase I footprinting was slightly higher compared to that measured by mobility shifts (46 versus 64 nM, respectively), and both values are significantly weaker than the affinity of GuNikR for $P_{nik(MN)1}$. Although the DNA binding site(s) and stoichiometry of the GuNikR-$P_{nik(MN)2}$ interaction are not fully resolved, apparent affinities for the interaction of

TABLE 1. Apparent DNA binding affinities of wild-type and N-terminal arm mutants of GuNikR[a]

Promoter	K_D (nM) ± SD; Hill coefficient ± SD[b]					
	Wild type		A2ins (EMSA)	G2A (EMSA)	E3A (EMSA)	T4A (EMSA)
	EMSA	DNase I				
nik(MN)1	7.6 ± 0.7; 1.61 ± 0.17	16.5 ± 3.8; 2.03 ± 0.55	86.1 ± 1.8; 0.99 ± 0.11	53.7 ± 8.6; 1.29 ± 0.19	76.7 ± 14.9; 0.95 ± 0.04	270.2 ± 8.8; 1.26 ± 0.08
nik(MN)2	64.4 ± 50.4; 0.60 ± 0.25	45.8 ± 19.3; 2.56 ± 0.09	≤2,000*; 1.36 ± 0.42	≤1,200*; 2.27 ± 1.73	99.8 ± 47.0; 0.93 ± 0.02	≤1,230*; 1.10 ± 0.28

[a] The apparent affinity was determined from fits of the data with the Hill equation. For *nik(MN)2*, the data were fit without differentiating distinct shifted species. Attempts to fit this data to a model with only two distinct binding sites (*K* values) were unsuccessful.
[b] *, Only the lower-limit estimate is given.

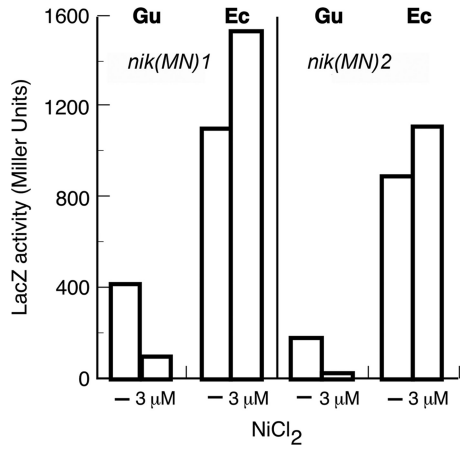

FIG. 4. GuNikR regulates expression from $P_{nik(MN)}$ promoters in a heterologous system. Promoter-*lacZ* fusions were cotransformed into *E. coli*, together with a plasmid expressing GuNikR or EcNikR. The LacZ activity was determined under aerobic growth conditions in M63 minimal medium containing no added $NiCl_2$ or 3 μM $NiCl_2$.

GuNikR with $P_{nik(MN)2}$ were determined by using the Hill equation to provide a basis for comparison with $P_{nik(MN)1}$, as well as for the interaction of GuNikR mutants with this DNA fragment.

***G. bemidjiensis* NikR binds to a 30-bp region of a *nik(MN)* candidate promoter.** The interaction of multiple GuNikR tetramers with $P_{nik(MN)1}$ was also supported by DNA binding assays with the closely related *G. bemidjiensis* NikR (GbNikR; Fig. 2a, 87% identical and 94% similar to GuNikR). In a mobility shift assay GbNikR specifically bound the upstream region (Fig. 3c) of a predicted *nik(MN)* gene (Gbem2225), one of four *nik(MN)* candidates identified in the *G. bemidjiensis* genome. Notably, the GbNikR-DNA complex exhibited a smaller mobility shift compared to GuNikR-$P_{nik(MN)1}$ and GuNikR-$P_{nik(MN)2}$. Furthermore, GbNikR protected a 30-bp region of the *nik(MN)* candidate promoter (Fig. 5a). Thus, the difference in size of the footprints and relative mobility shifts for GbNikR and GuNikR support the idea that GuNikR binds to both $P_{nik(MN)1}$ and $P_{nik(MN)2}$ as a higher-order complex, most likely two NikR tetramers per candidate promoter.

The two GuNikR binding sites in $P_{nik(MN)1}$ are not equivalent. The 70-bp region of $P_{nik(MN)1}$ protected by GuNikR spanned two imperfect inverted repeats (GACATAC–13 bp–GTATTCA–4 bp–GTGCTAC–13 bp–GTGTTAC; Fig. 5c). A sequence similar to the downstream *nik(MN)1* inverted repeats is also present in the *nik(MN)2* promoter region, and the *nikMN* upstream region from several other *Geobacter* species, including *G. bemidjiensis* (Fig. 5c). These sequences all contain a putative −35 consensus sequence (TTGACA) for RpoD/RpoS recognition (48).

Poorly conserved inverted repeats, like the upstream sequence found in $P_{nikMN(1)}$ are present in $P_{nik(MN)2}$ (GTGATGA–13 bp–AGGCTAC, 9 bp downstream of the DNase I footprint) and in Gb-$P_{nik(MN)}$-(GTGCTAT–9 bp–GTATATC, upstream of the DNase I footprint). In the latter case, however, the sequence contains several mismatches, and the spacing between half sites is significantly shorter (Fig. 5c).

The less conserved inverted repeat sequences in $P_{nik(MN)1}$ and $P_{nik(MN)2}$ are likely candidates for binding of a second GuNikR tetramer. However, the spacing between the two sets of potential repeats at $P_{nik(MN)2}$ is different from that at $P_{nik(MN)1}$ (9 bp versus 4 bp). Based on the footprinting and mobility shift data, it appears that the larger spacing in $P_{nik(MN)2}$ is suboptimal for GuNikR binding.

The relative contributions of each pair of repeats in $P_{nik(MN)1}$ to GuNikR binding were assessed by mutation of the inverted repeat sequences. The site 1 (upstream) or site 2 (downstream) sequences were scrambled by changing pyrimidines to purines and vice versa. These sequence changes eliminated the predicted inverted repeat sequences and did not create new potential GuNikR binding sites. The effect of each site mutation on GuNikR binding was determined by using mobility shift assays. Scrambling $P_{nik(MN)1}$ site 1 had little effect on GuNikR affinity (K_D = 5.8 ±0.1 nM), but cooperativity was substantially reduced (n = 1.1), which was consistent with the observation of a complex with intermediate mobility. In contrast, scrambling $P_{nik(MN)1}$ site 2 severely reduced GuNikR affinity (>80-fold), as evidenced by the persistence of the free DNA species at high protein concentrations, as well as the absence of any substantial population of the shifted species. A lower limit for the affinity of this interaction was estimated to be ~600 nM. These results support different contributions of sites 1 and 2 to GuNikR-$P_{nik(MN)1}$ binding, wherein GuNikR bound to site 2 is a high-affinity interaction and GuNikR bound to site 1 is a weak interaction that is strongly stabilized by the presence of GuNikR bound to site 2.

The N-terminal arm of GuNikR is required for DNA binding. To further explore GuNikR interactions with $P_{nik(MN)1}$ and $P_{nik(MN)2}$, residues N terminal to the GuNikR Arg-Gly-Ser β-sheet were mutated to assess their contributions to DNA binding affinity and cooperativity. We created an N-terminal arm truncation mutant of GuNikR (Δnt3GuNikR), as well as individual Ala substitutions, which is analogous to our previous study of HpNikR (6). Truncation of the arm did not affect protein folding, since there was no significant difference between the CD spectra of full-length and Δnt3GuNikR (see Fig. S3 in the supplemental material). The individual Ala mutations also did not affect protein folding (data not shown).

Δnt3GuNikR was unable to bind $P_{nik(MN)1}$ or $P_{nik(MN)2}$ DNA at protein concentrations up to 5 μM in either DNase I footprinting or mobility shift assays (data not shown). These results demonstrate that the N-terminal arm of GuNikR is essential for DNA binding, which contrasts with the role of the N-terminal arm of HpNikR (6, 28). Truncation of the nine-residue arm of HpNikR did not alter the affinity of the protein for promoters that it binds tightly but increased the affinity of weaker or nonspecific DNA interactions (6, 28).

To identify contributions of specific residues of the GuNikR N-terminal arm to DNA binding, we measured the DNA affinity of the Ala mutants using mobility shifts. In addition to the individual amino acid substitutions, a fourth mutant was created by inserting an Ala codon immediately following the N-terminal Met codon to create Ala2ins (arm sequence of AGETI after cleavage of the N-terminal Met residue [24]). This substitution will affect the position of the NH_2 terminus of the protein and provides a way to assess its contribution to DNA binding. Mobility shift assays of each GuNikR mutant with $P_{nik(MN)1}$ and $P_{nik(MN)2}$ demonstrated that various contributions are made from each residue to DNA binding affinity

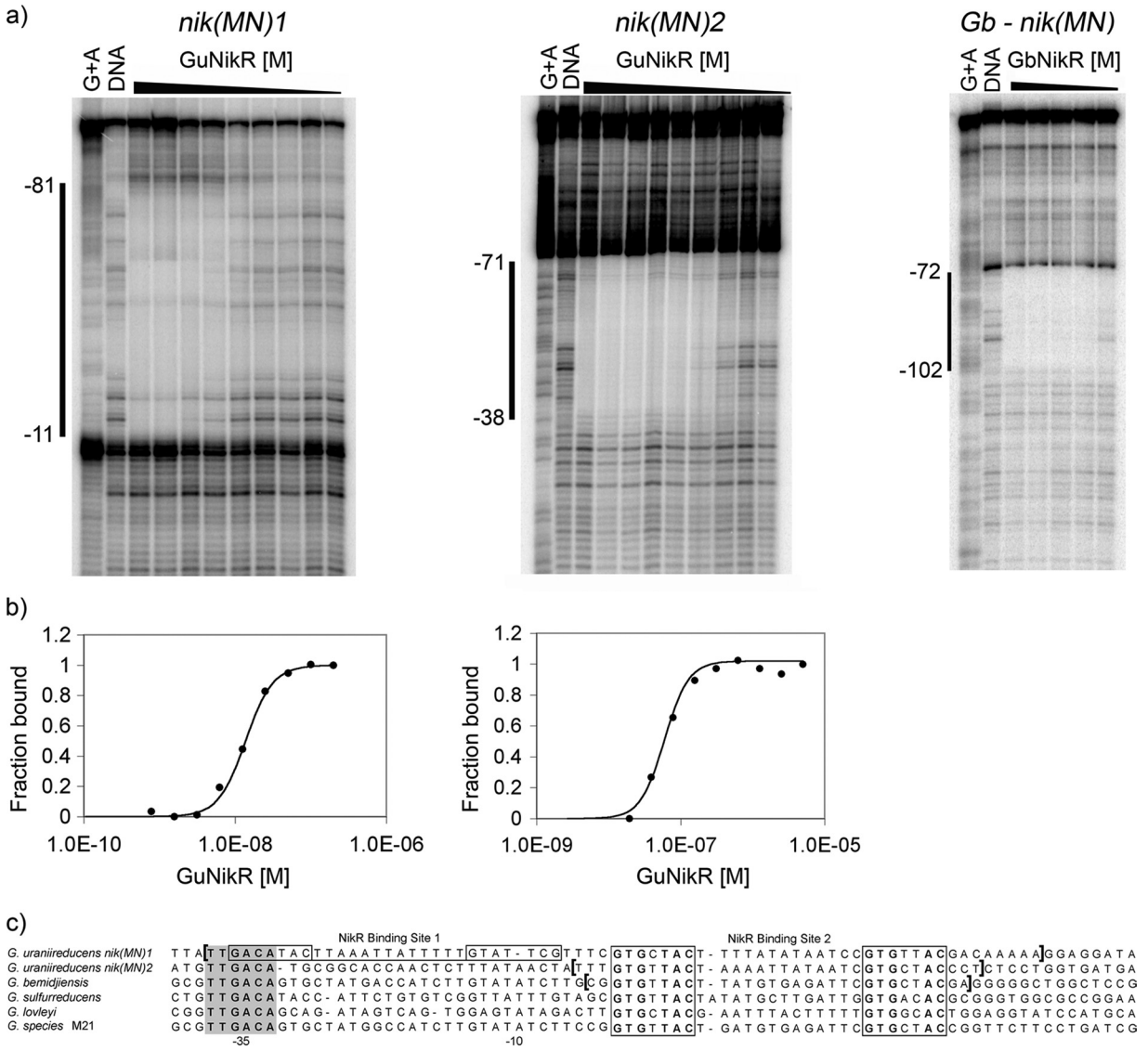

FIG. 5. GuNikR recognizes two pairs of repeats at $P_{nik(MN)1}$, and GuNikR and GbNikR recognize one pair of repeats at $P_{nik(MN)2}$ and $P_{Gb\text{-}nik(MN)}$, respectively. (a) DNase I footprinting of GuNikR serially diluted 2-fold from 500 nM to 2 nM with $P_{nik(MN)1}$ or from 5 μM to 20 nM with $P_{nik(MN)2}$ and GbNikR serially diluted 3-fold from 5.0 μM to 62 nM with $P_{Gb\text{-}nik(MN)}$. All titrations were performed in the presence of stoichiometric $NiCl_2$. (b) Fraction of bound $P_{nik(MN)1}$ or $P_{nik(MN)2}$ with increasing GuNikR concentration as determined by quantitation of the gels shown in panel a. (c) Predicted $P_{nik(MN)}$ promoter sequences from different *Geobacter* species. The putative −35 TTGACA promoter element is shaded, and the bases are indicated in boldface. The DNA footprints for $P_{nik(MN)1}$, $P_{nik(MN)2}$, and $P_{Gb\text{-}nik(MN)}$ are indicated by brackets. The DNA recognition motif recognized by GuNikR is boxed, and conserved residues are indicated in boldface. The predicted second NikR binding site in $P_{nik(MN)1}$ (site 1) is underlined, and weakly conserved candidate inverted repeat sequences are boxed.

and specificity (Fig. 6b to e and Table 1). Furthermore, these contributions are different for each candidate promoter. Except for Glu3Ala, all of the mutations strongly affected GuNikR binding to $P_{nik(MN)2}$. The effect of the Ala2ins mutation suggests a specific structural role for the NH_2 terminus of the protein in DNA recognition.

For $P_{nik(MN)1}$ no mutation resulted in the loss of the low-mobility species or the presence of an intermediate mobility species, which was observed for the scrambled candidate promoter mutants. However, quantitation of the loss of the free DNA species and changes in the abundance of an intermediate shifted band suggested that these mutants affect the cooperativity of GuNikR binding to $P_{nik(MN)1}$. In addition, the arm mutations all reduced DNA binding affinity to some extent, with Thr4Ala being the most severely affected mutant. The difficulty of assigning affinities to the two sites of $P_{nik(MN)1}$ using these assays precludes quantitatively determining individual contributions to cooperativity and DNA binding affinity, but it is clear that each arm residue is important for GuNikR DNA binding.

DISCUSSION

The results presented here identify a new mode of NikR-DNA recognition. We have shown that GuNikR tetramers

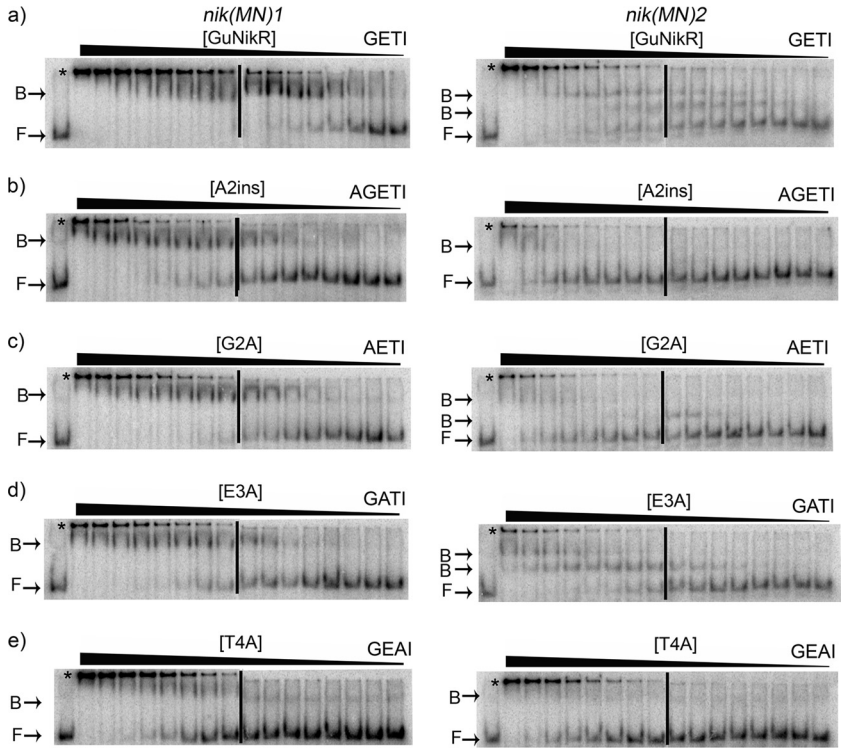

FIG. 6. GuNikR requires each N-terminal arm residue for high-affinity DNA binding. Wild-type GuNikR (a; same as in Fig. 3) or N-terminal site mutants A2ins (b), G2A (c), E3A (d), and T4A (e) were serially diluted 1.7-fold from 5.0 μM to 17.5 nM with $P_{nik(MN)1}$ (left panels) or $P_{nik(MN)2}$ (right panels). Each arm sequence is indicated to the upper right of each pair of gels. Mobility shifts were performed with 50 μM $NiCl_2$ in the gel and running buffer. Each full titration was run on two separate gels in parallel, and a vertical line separates each pair of gel images. F, free DNA. B, protein-bound DNA. The asterisk indicates DNA in wells.

bind with positive cooperativity to the *nik(MN)1* promoter. In addition, GuNikR utilizes amino acids N-terminal to its β-sheet motif for stable DNA complex formation. Some of these residues are also linked to cooperative tetramer binding. The importance of these residues is distinct from that of the HpNikR N-terminal arm, which is not essential for DNA-binding but is a major determinant of sequence specific DNA binding (6, 28).

GuNikR protection of $P_{nik(MN)1}$ is significantly larger than the 40 and 36 bp protected by EcNikR (11) and HpNikR (1, 6, 17, 22), respectively. Although GuNikR protected a smaller region of $P_{nik(MN)2}$, there are additional poorly conserved repeats in this candidate promoter, suggesting that the multiple shifted complexes observed in mobility shift assays of GuNikR with $P_{nik(MN)2}$ represent higher-order protein-DNA complexes. The smaller mobility shift and footprint for the GbNikR-$P_{nik(MN)}$ interaction further suggests that multiple GuNikR tetramers binding to $P_{nik(MN)2}$ may be obscured in the footprinting experiment, possibly due to the presence of multiple binding sites for which GuNikR has low affinity.

Together with the significant positive cooperativity observed for GuNikR binding to both *nik(MN)* promoter fragments, these results argue that two GuNikR tetramers bind to $P_{nik(MN)1}$ and $P_{nik(MN)2}$. This represents a surprisingly distinct mode of DNA binding compared to previously characterized NikR family members.

The molecular basis for GuNikR cooperative DNA binding to $P_{nik(MN)1}$ remains to be determined. The arrangement of GuNikR recognition motifs at $P_{nik(MN)1}$ and the observed footprint argues against a model analogous to the iron-dependent DtxR-DNA interaction, wherein two repressor molecules bind cooperatively, but on opposite faces of the DNA, and generate a footprint like that expected for a single repressor molecule (9, 47). Sites 1 and 2 of $P_{nik(MN)1}$ are separated by 4 bp, which means the centers of the closest half-sites are separated by 12 bp and the GuNikR tetramers will be adjacent to each other on the same side of the DNA. Based on the cocrystal structure of EcNikR bound to the *nikA* promoter (40), the spacing between the closest half-sites of site 1 and site 2 suggests two possible modes of cooperativity. In one case, the two GuNikR tetramers contact one another via residues of the RHH dimers that sit in adjacent major grooves. Alternatively, GuNikR bound to Site 2 could distort the DNA helix and allow a second tetramer to bind to Site 1. Cooperativity by DNA distortion in the absence of protein-protein interactions has been demonstrated (30). The greater spacing between the two inverted repeat sequences detected in $P_{nik(MN)2}$ likely decreases cooperativity either by disrupting the interactions between two GuNikR tetramers or by diminishing the effect of any DNA distortion upon binding of the first GuNikR tetramer.

Little is known about the role of nickel ions in *Geobacter* physiology. Molecular hydrogen can serve as an electron source for dissimilatory metal reduction (29). Changes in [Ni-Fe] hydrogenase gene expression levels have been detected in cells grown in defined culture relative to cells grown in sediment from which the strains were isolated (26). Although the

repression of nickel transport genes by GuNikR is not surprising, the nature of the GuNikR-$P_{nik(MN)1}$ and -$P_{nik(MN)2}$ complexes may have direct implications for nickel-dependent gene regulation in *G. uraniireducens*. Because cooperative DNA binding by GuNikR increases the affinity of the second tetramer for DNA, the concentration of GuNikR, and thus nickel, required for DNA occupancy and repression by GuNikR is decreased relative to the tetrameric EcNikR-DNA interaction. The predicted Nik(MN) protein sequences are 84% identical and, combined with the different relative expression levels of the $P_{nik(MN)}$-*lacZ* fusions, lead us to speculate that the two Nik(MN) proteins may have different functional roles. The availability of genetic tools for *Geobacter* species (29) will facilitate dissection of the function of each Nik(MN) protein and their patterns of nickel- and NikR-dependent gene regulation.

A second notable feature of the GuNikR (and GbNikR)-DNA interactions is the primary recognition sequence, GTG(T/C)TAC–13 bp–GTG(C/T)TAC. The 7-bp repeats can be viewed either as inverted repeats that are conserved at the external positions (GTXXXAC) or as highly conserved direct repeats, although the former seems most likely. Interestingly, the inverted repeats recognized by EcNikR can also be extended to 7 bp with the indicated underlined bases (GTATGAC–14 bp–GTCATAC). This addition generates the analogous direct repeat sequence found for the *Geobacter* NikRs, but with less conservation of the central residues for the two repeats in the case of EcNikR. The structure of the EcNikR-DNA complex clearly shows recognition of inverted repeats as the EcNikR β-sheet residues do not directly contact the innermost C-G and G-C bps of the 7-bp sequences (40). Interestingly, the bioinformatics study that predicted various NikR binding motifs indicated that the inner bases of the extended EcNikR motif are not conserved in the Arg-Thr-Thr β-sheet family (35). Conversely, the 7-bp half site sequences of a subset of the Arg-Gly-Ser β-sheet containing NikRs, including those from *Geobacter* species, are conserved. Further studies will be required to identify the nature of the specific contacts between GuNikR and its operator sequences.

A common feature of nearly all NikR homologs is an Arg residue at the first position of the β-sheet. In EcNikR, this residue dominates the direct contacts between the protein and DNA (40), but in an asymmetric fashion, since only one of the two Arg residues in an RHH dimer makes direct DNA contacts. The sequences of the repeats recognized by GuNikR identified here suggest that this pattern of Arg-DNA contacts is not completely conserved throughout the NikR family. The half-site repeats recognized by GuNikR begin and end with G-T base pairs similar to those contacted by Arg3 of EcNikR (40). However, the N-terminal arm also makes significant contributions to GuNikR-DNA interactions. The severe effects of the Thr4Ala substitution on binding affinity for both the *nik(MN)1* and the *nik(MN)2* candidate promoters, together with the polar nature of the Thr side chain, suggest that this residue either makes direct contacts with the DNA or helps to orient the β-sheet for DNA binding. Thr4 likely compensates for the absence of a polar residue in the middle of the GuNikR β-sheet (Arg-Gly-Ser), which corresponds to the middle sheet position of EcNikR (Thr5) that makes a direct contact with the operator sequence (40). The extension of specific DNA interactions with protein residues outside the β-sheet could account for the apparently larger half site sequence that is predicted to be recognized by GuNikR. Mutation of the Gly residue was not attempted here because any amino acid substitution will likely perturb the β-sheet conformation because of the unique conformational properties of glycine.

The results presented here affirm the prediction of NikR DNA recognition motifs using a bioinformatics approach (35). However, some NikR recognition motifs remain poorly defined. The bioinformatics approach was not able to predict a DNA binding motif for the structurally characterized *Pyrococcus horikoshii* NikR (14). In addition, experimental studies of the sequence dependence of HpNikR-DNA interactions (1, 6, 17, 22) show little similarity to the predicted DNA recognition motif for HpNikR (35).

NikR DNA binding activity and gene regulation is likely influenced by each organism's nickel physiology. Of the three NikR proteins for which DNA binding has been characterized, there are distinct features for each that have regulatory implications. For EcNikR, there is biochemical evidence for the role of two types of nickel-binding site in regulating DNA binding affinity (8, 12). Thus far, EcNikR is the only ortholog for which this effect has been observed. However, the biological roles of these two sites have not yet been uncoupled so their individual contributions to the regulation of gene expression is unclear. HpNikR recognizes several promoter regions and thus will influence nickel utilization by controlling the expression of more genes than just those required for nickel import.

Currently, it appears that the complexity of HpNikR-dependent gene regulation is due in part to differential roles of residues in the N-terminal arm of the protein in DNA binding (6). These conformational differences may be linked to changes in intracellular physiology (28). Here, we have shown the potential for influencing NikR-dependent gene regulation by exploiting cooperative interactions between NikR tetramers. Undoubtedly, the majority of NikR proteins will share common regulatory features with one of the three proteins already characterized. Nonetheless, it is intriguing that significant variability exists in the nickel- and DNA-binding properties of different NikR proteins. These differences provide insight into the evolution of DNA binding by the NikR family.

ACKNOWLEDGMENTS

This study was supported by National Science Foundation grant MCB0520877.

We thank Evgenya Shelobolina and Derek Lovley for the generous gifts of genomic DNA.

REFERENCES

1. **Abraham, L. O., Y. Li, and D. B. Zamble.** 2006. The metal- and DNA-binding activities of *Helicobacter pylori* NikR. J. Inorg. Biochem. **100:**1005–1014.
2. **Altschul, S. F., T. L. Madden, A. A. Schaffer, J. Zhang, Z. Zhang, W. Miller, and D. J. Lipman.** 1997. Gapped BLAST and PSI-BLAST: a new generation of protein database search programs. Nucleic Acids Res. **25:**3389–3402.
3. **Anderson, R. T., H. A. Vrionis, I. Ortiz-Bernad, C. T. Resch, P. E. Long, R. Dayvault, K. Karp, S. Marutzky, D. R. Metzler, A. Peacock, D. C. White, M. Lowe, and D. R. Lovley.** 2003. Stimulating the *in situ* activity of *Geobacter* species to remove uranium from the groundwater of a uranium-contaminated aquifer. Appl. Environ. Microbiol. **69:**5884–5891.
4. **Ballantine, S. P., and D. H. Boxer.** 1985. Nickel-containing hydrogenase isoenzymes from anaerobically grown *Escherichia coli* K-12. J. Bacteriol. **163:**454–459.
5. **Benanti, E. L., and P. T. Chivers.** 2009. An intact urease assembly pathway

is required to compete with NikR for nickel ions in *Helicobacter pylori*. J. Bacteriol. **191:**2405–2408.
6. **Benanti, E. L., and P. T. Chivers.** 2007. The N-terminal arm of the *Helicobacter pylori* Ni^{2+}-dependent transcription factor NikR is required for specific DNA binding. J. Biol. Chem. **282:**20365–20375.
7. **Berggrun, A., and R. T. Sauer.** 2000. Interactions of Arg2 in the Mnt N-terminal arm with the central and flanking regions of the Mnt operator. J. Mol. Biol. **301:**959–973.
8. **Bloom, S. L., and D. B. Zamble.** 2004. Metal-selective DNA-binding response of *Escherichia coli* NikR. Biochemistry **43:**10029–10038.
9. **Chen, C. S., A. White, J. Love, J. R. Murphy, and D. Ringe.** 2000. Methyl groups of thymine bases are important for nucleic acid recognition by DtxR. Biochemistry **39:**10397–10407.
10. **Chen, Y. Y., and R. A. Burne.** 2003. Identification and characterization of the nickel uptake system for urease biogenesis in *Streptococcus salivarius* 57.I. J. Bacteriol. **185:**6773–6779.
11. **Chivers, P. T., and R. T. Sauer.** 1999. NikR is a ribbon-helix-helix DNA-binding protein. Protein Sci. **8:**2494–2500.
12. **Chivers, P. T., and R. T. Sauer.** 2002. NikR repressor: high-affinity nickel binding to the C-terminal domain regulates binding to operator DNA. Chem. Biol. **9:**1141–1148.
13. **Chivers, P. T., and R. T. Sauer.** 2000. Regulation of high-affinity nickel uptake in bacteria. Ni^{2+}-Dependent interaction of NikR with wild-type and mutant operator sites. J. Biol. Chem. **275:**19735–19741.
14. **Chivers, P. T., and T. H. Tahirov.** 2005. Structure of *Pyrococcus horikoshii* NikR: nickel sensing and implications for the regulation of DNA recognition. J. Mol. Biol. **348:**597–607.
15. **Contreras, M., J. M. Thiberge, M. A. Mandrand-Berthelot, and A. Labigne.** 2003. Characterization of the roles of NikR, a nickel-responsive pleiotropic autoregulator of *Helicobacter pylori*. Mol. Microbiol. **49:**947–963.
16. **Davis, G. S., E. L. Flannery, and H. L. Mobley.** 2006. *Helicobacter pylori* HP1512 is a nickel-responsive NikR-regulated outer membrane protein. Infect. Immun. **74:**6811–6820.
17. **Delany, I., R. Ieva, A. Soragni, M. Hilleringmann, R. Rappuoli, and V. Scarlato.** 2005. *In vitro* analysis of protein-operator interactions of the NikR and fur metal-responsive regulators of coregulated genes in *Helicobacter pylori*. J. Bacteriol. **187:**7703–7715.
18. **De Pina, K., V. Desjardin, M. A. Mandrand-Berthelot, G. Giordano, and L. F. Wu.** 1999. Isolation and characterization of the *nikR* gene encoding a nickel-responsive regulator in *Escherichia coli*. J. Bacteriol. **181:**670–674.
19. **Dosanjh, N. S., N. A. Hammerbacher, and S. L. Michel.** 2007. Characterization of the *Helicobacter pylori* NikR-P(*ureA*) DNA interaction: metal ion requirements and sequence specificity. Biochemistry **46:**2520–2529.
20. **Dosanjh, N. S., A. L. West, and S. L. Michel.** 2009. *Helicobacter pylori* NikR's interaction with DNA: a two-tiered mode of recognition. Biochemistry **48:**527–536.
21. **Eckert, R. L.** 2001. DNA sequencing by the chemical method. John Wiley & Sons, Inc., New York, NY. doi:10.1002/0471142727.mb0705s17. [Online.]
22. **Ernst, F. D., E. J. Kuipers, A. Heijens, R. Sarwari, J. Stoof, C. W. Penn, J. G. Kusters, and A. H. van Vliet.** 2005. The nickel-responsive regulator NikR controls activation and repression of gene transcription in *Helicobacter pylori*. Infect. Immun. **73:**7252–7258.
23. **Ernst, F. D., J. Stoof, W. M. Horrevoets, E. J. Kuipers, J. G. Kusters, and A. H. van Vliet.** 2006. NikR mediates nickel-responsive transcriptional repression of the *Helicobacter pylori* outer membrane proteins FecA3 (HP1400) and FrpB4 (HP1512). Infect. Immun. **74:**6821–6828.
24. **Frottin, F., A. Martinez, P. Peynot, S. Mitra, R. C. Holz, C. Giglione, and T. Meinnel.** 2006. The proteomics of N-terminal methionine cleavage. Mol. Cell Proteomics **5:**2336–2349.
25. **Gasteiger, E., H. C. A. Gattiker, S. Duvaud, M. R. Wilkins, R. D. Appel, and A. Bairoch.** 2005. Protein identification and analysis tools on the ExPASy Server. *In* The proteomics protocols handbook. Humana Press, Inc., New York, NY.
26. **Holmes, D. E., R. A. O'Neil, M. A. Chavan, L. A. N′Guessan, H. A. Vrionis, L. A. Perpetua, M. J. Larrahondo, R. DiDonato, A. Liu, and D. R. Lovley.** 2009. Transcriptome of *Geobacter uraniireducens* growing in uranium-contaminated subsurface sediments. ISME J. **3:**216–230.
27. **Leitch, S., M. J. Bradley, J. L. Rowe, P. T. Chivers, and M. J. Maroney.** 2007. Nickel-specific response in the transcriptional regulator, *Escherichia coli* NikR. J. Am. Chem. Soc. **129:**5085–5095.
28. **Li, Y., and D. Zamble.** 2009. The pH-responsive DNA-binding activity of *Helicobacter pylori* NikR. Biochemistry **48:**2486–2496.
29. **Lovley, D. R., D. E. Holmes, and K. P. Nevin.** 2004. Dissimilatory Fe(III) and Mn(IV) reduction. Adv. Microb. Physiol. **49:**219–286.
30. **Moretti, R., L. J. Donato, M. L. Brezinski, R. L. Stafford, H. Hoff, J. S. Thorson, P. B. Dervan, and A. Z. Ansari.** 2008. Targeted chemical wedges reveal the role of allosteric DNA modulation in protein-DNA assembly. ACS Chem. Biol. **3:**220–229.
31. **Mulrooney, S. B., and R. P. Hausinger.** 2003. Nickel uptake and utilization by microorganisms. FEMS Microbiol. Rev. **27:**239–261.
32. **Navarro, C., L. F. Wu, and M. A. Mandrand-Berthelot.** 1993. The *nik* operon of *Escherichia coli* encodes a periplasmic binding-protein-dependent transport system for nickel. Mol. Microbiol. **9:**1181–1191.
33. **Postle, K., and R. A. Larsen.** 2007. TonB-dependent energy transduction between outer and cytoplasmic membranes. Biometals **20:**453–465.
34. **Raumann, B. E., B. M. Brown, and R. T. Sauer.** 1994. Major groove DNA recognition by β-sheets: the ribbon-helix-helix family of gene regulatory proteins. Curr. Opin. Struct. Biol. **4:**36–43.
35. **Rodionov, D. A., P. Hebbeln, M. S. Gelfand, and T. Eitinger.** 2006. Comparative and functional genomic analysis of prokaryotic nickel and cobalt uptake transporters: evidence for a novel group of ATP-binding cassette transporters. J. Bacteriol. **188:**317–327.
36. **Rowe, J. L., G. L. Starnes, and P. T. Chivers.** 2005. Complex transcriptional control links NikABCDE-dependent nickel transport with hydrogenase expression in *Escherichia coli*. J. Bacteriol. **187:**6317–6323.
37. **Sawers, R. G., S. P. Ballantine, and D. H. Boxer.** 1985. Differential expression of hydrogenase isoenzymes in *Escherichia coli* K-12: evidence for a third isoenzyme. J. Bacteriol. **164:**1324–1331.
38. **Schauer, K., B. Gouget, M. Carriere, A. Labigne, and H. de Reuse.** 2007. Novel nickel transport mechanism across the bacterial outer membrane energized by the TonB/ExbB/ExbD machinery. Mol. Microbiol. **63:**1054–1068.
39. **Schreiter, E. R., M. D. Sintchak, Y. Guo, P. T. Chivers, R. T. Sauer, and C. L. Drennan.** 2003. Crystal structure of the nickel-responsive transcription factor NikR. Nat. Struct. Biol. **10:**794–799.
40. **Schreiter, E. R., S. C. Wang, D. B. Zamble, and C. L. Drennan.** 2006. NikR-operator complex structure and the mechanism of repressor activation by metal ions. Proc. Natl. Acad. Sci. U. S. A. **103:**13676–13681.
41. **Shelobolina, E. S., H. A. Vrionis, R. H. Findlay, and D. R. Lovley.** 2008. *Geobacter uraniireducens* sp. nov., isolated from subsurface sediment undergoing uranium bioremediation. Int. J. Syst. Evol. Microbiol. **58:**1075–1078.
42. **Somers, W. S., and S. E. Phillips.** 1992. Crystal structure of the met repressor-operator complex at 2.8 Å resolution reveals DNA recognition by beta-strands. Nature **359:**387–393.
43. **Thompson, J. D., D. G. Higgins, and T. J. Gibson.** 1994. CLUSTAL W: improving the sensitivity of progressive multiple sequence alignment through sequence weighting, position-specific gap penalties and weight matrix choice. Nucleic Acids Res. **22:**4673–4680.
44. **Tomb, J. F., O. White, A. R. Kerlavage, R. A. Clayton, G. G. Sutton, R. D. Fleischmann, K. A. Ketchum, H. P. Klenk, S. Gill, B. A. Dougherty, K. Nelson, J. Quackenbush, L. Zhou, E. F. Kirkness, S. Peterson, B. Loftus, D. Richardson, R. Dodson, H. G. Khalak, A. Glodek, K. McKenney, L. M. Fitzegerald, N. Lee, M. D. Adams, E. K. Hickey, D. E. Berg, J. D. Gocayne, T. R. Utterback, J. D. Peterson, J. M. Kelley, M. D. Cotton, J. M. Weidman, C. Fujii, C. Bowman, L. Watthey, E. Wallin, W. S. Hayes, M. Borodovsky, P. D. Karp, H. O. Smith, C. M. Fraser, and J. C. Venter.** 1997. The complete genome sequence of the gastric pathogen *Helicobacter pylori*. Nature **388:**539–547.
45. **Unden, G., and J. Bongaerts.** 1997. Alternative respiratory pathways of *Escherichia coli*: energetics and transcriptional regulation in response to electron acceptors. Biochim. Biophys. Acta **1320:**217–234.
46. **Wang, S. C., A. V. Dias, and D. B. Zamble.** 2009. The "metallo-specific" response of proteins: a perspective based on the *Escherichia coli* transcriptional regulator NikR. Dalton Trans. **2009:**2459–2466.
47. **White, A., X. Ding, J. C. vanderSpek, J. R. Murphy, and D. Ringe.** 1998. Structure of the metal-ion-activated diphtheria toxin repressor/tox operator complex. Nature **394:**502–506.
48. **Yan, B., C. Nunez, T. Ueki, A. Esteve-Nunez, M. Puljic, R. M. Adkins, B. A. Methe, D. R. Lovley, and J. Krushkal.** 2006. Computational prediction of RpoS and RpoD regulatory sites in *Geobacter sulfurreducens* using sequence and gene expression information. Gene **384:**73–95.
49. **Zhang, Y., D. A. Rodionov, M. S. Gelfand, and V. N. Gladyshev.** 2009. Comparative genomic analyses of nickel, cobalt and vitamin B12 utilization. BMC Genomics **10:**78.